Generalized constrained energy minimization approach to subpixel target detection for multispectral imagery

Chein-I Chang, MEMBER SPIE
University of Maryland—Baltimore County
Department of Computer Science
and Electrical Engineering
Baltimore, Maryland 21250
E-mail: cchang@umbc.edu

Jih-Ming Liu
Bin-Chang Chieu
National Taiwan Science and Technology
University
Department of Electrical Engineering
Taipei, Taiwan

Hsuan Ren
University of Maryland—Baltimore County
Department of Computer Science
and Electrical Engineering
Baltimore, Maryland 21250

Chuin-Mu Wang
Chien-Shun Lo
Pau-Choo Chung
National Cheng-Kung University
Department of Electrical Engineering
Tainan, Taiwan

Ching-Wen Yang
Taichung Veterans General Hospital
Computer Center
Taichung, Taiwan

Dye-Jyun Ma
National Chung-Hsing University
Taichung, Taiwan

Abstract. Subpixel detection in multispectral imagery presents a challenging problem due to relatively low spatial and spectral resolution. We present a generalized constrained energy minimization (GCEM) approach to detecting targets in multispectral imagery at subpixel level. GCEM is a hybrid technique that combines a constrained energy minimization (CEM) method developed for hyperspectral image classification with a dimensionality expansion (DE) approach resulting from a generalized orthogonal subspace projection (GOSP) developed for multispectral image classification. DE enables us to generate additional bands from original multispectral images nonlinearly so that CEM can be used for subpixel detection to extract targets embedded in multispectral images. CEM has been successfully applied to hyperspectral target detection and image classification. Its applicability to multispectral imagery is yet to be investigated. A potential limitation of CEM on multispectral imagery is the effectiveness of interference elimination due to the lack of sufficient dimensionality. DE is introduced to mitigate this problem by expanding the original data dimensionality. Experiments show that the proposed GCEM detects targets more effectively than GOSP and CEM without dimensionality expansion. [S0091-3286(00)01205-8]

Subject terms: classification; constrained energy minimization; dimensionality expansion; generalized constrained energy minimization; generalized orthogonal subspace projection; hyperspectral image; multispectral image; subpixel detection.

Paper ATR-013 received Sep. 3, 1999; revised manuscript received Nov. 23, 1999; accepted for publication Dec. 9, 1999.

1 Introduction

Multispectral images differ from hyperspectral images in the sense that the former is acquired by tens of spectral bands (channels) compared to the latter by hundreds of spectral bands. Such low spectral resolution resulting from a small number of spectral bands presents a challenging problem for subpixel detection and classification in multispectral imagery. Intuitively, if there are m materials or endmembers, it requires at least n spectral bands with $n > m$ to produce satisfactory classification results. This phenomenon was demonstrated in Ref. 1 and is referred to the band number constraint (BNC). More precisely, it requires at least more than m spectral bands to classify m endmembers so that each endmember can be diagnosed by a separate spectral band. This fact is similar to the well-known pigeon-hole principle in discrete mathematics.[2] To resolve this issue, Ren and Chang[3] recently proposed a generalized orthogonal subspace projection (GOSP) approach, which developed a band generation process to produce additional images so that the original multispectral imagery can be expanded. These newly generated images are produced by making use of various nonlinear correlations among a given set of original multispectral images. Combining these extra generated images with the original images results in sufficient dimensions that can be used to accommodate more material substances that must be classified. However, there is also a trade-off due to such image data expansion. Some unwanted signatures may be also generated and mix with the material signatures of interest. These undesired signatures are usually not known *a priori*. Therefore, many existing mixed pixel classification methods such as orthogonal subspace projection (OSP)-based classifier[3,4] and maximum likelihood classifier,[5,6] may not be appropriate because they require a complete knowledge of material signatures present in images.

To alleviate the requirement of prior knowledge about material signatures, a recent approach, called constrained energy minimization (CEM) was proposed.[7–9] The idea of CEM arises in Frost's linearly constrained adaptive beamforming approach developed for array processing.[10] It first selects a material signature as a target signature to be detected and classified. Since the target signature is the only signature we are interested in, we could design an adaptive filter to pass the desired target with a specific gain while the filter output resulting from unknown signal sources can be minimized. To accomplish this task, CEM interpreted the target signature of interest as the signal arrived from a desired direction in the context of a linearly constrained minimum variance (LCMV) beamforming problem[10–12] so that finding a CEM filter is equivalent to seeking an adaptive beamformer, which locks on the desired direction of signal arrival with a specific constraint. The weights chosen for the desired adaptive beamformer minimizes its output variance (or energy) subject to this specific response constraint. As a consequence, the effects of signals from directions other than the desired one is minimized. When the specific gain is chosen to be unity, the LCMV beamformer becomes the minimum variance distortionless response (MVDR) beamformer, which is the precise model on which CEM is based. Using the same approach carried out by the MVDR beamformer, a CEM-based detector was designed by a finite impulse response (FIR) filter in a similar fashion so that the desired target was passed through the filter while energies caused by the unknown signal sources were minimized.[7] For the purpose of simplicity, the term of CEM is referred throughout this paper to either a CEM-based detector or the CEM approach, depending on the context.

To use CEM for target detection, the data dimensionality must be sufficiently large. For a multispectral image its data dimensionality is generally too small to make CEM effective. In this paper, we combine CEM with a dimensionality expansion (DE) approach that was developed[3] in GOSP to derive a generalized CEM (GCEM) that can extend the target capability of CEM to multispectral images. The process of GCEM can be briefly described as follows. It first uses DE to produce a new set of nonlinearly correlated images from the original multispectral images to expand data dimensionality. It is important to note that images generated by linear correlation do not provide any new information for CEM since CEM is a linear FIR filter. The concept of creating nonlinearly correlated images can be traced back to multivariate analysis where a data correlation matrix is generally used to capture the second-order statistics of the data. Recently, this idea was also applied to create new samples for target detection and classification in hyperspectral images,[13] where only very few training samples were available for each target of interest and the data dimensionality was relatively large compared to the number of samples that could be used for training. In this case, the data sample correlation matrix was generally not of full rank. To resolve this problem, a new set of correlated samples was generated by the training samples using nonlinear correlation functions, e.g., autocorrelation and cross-correlation. Thus, by incorporating these newly generated nonlinear-correlated images into the original image data, the original data dimensionality is augmented in the sense that the number of spectral band images that can be used for data analysis is increased. With taking advantage of this new augmented set of images CEM can effectively eliminate unknown interference and undesired signal sources. This will be demonstrated by experiments conducted in this paper using a three-band SPOT (*Le Systeme Pour l'Observation de la Terra* Earth Observation System) image scene. The experimental results show that GCEM greatly improves CEM with no data dimensionality expansion. In order to further evaluate the performance of GCEM, GCEM is also compared[3] to GOSP. The experimental results also show that GCEM performs better than GOSP.

The remainder of this paper is organized as follows. Section 2 describes an approach, referred to as DE derived[2] from GOSP. Section 3 briefly reviews the CEM approach, then we present GCEM in Sec. 4. Section 5 reports a set of experiments conducted to evaluate the effectiveness of GCEM in classification performance using SPOT images for analysis. Section 6 presents some concluding comments.

2 DE

The idea of the DE approach presented in this section arises from a fact that a second-order random process is generally specified by its first-order and second-order statistics. If we view the original spectral band images as the first-order images, we can generate a set of second-order statistics spectral band images by capturing nonlinear correlations between these spectral band images. These correlated images generated by second-order statistics provide useful nonlinear correlation information about spectral band images that is missing in the set of the original spectral band images. The desired second-order statistics used for DE include autocorrelation, cross-correlation, and nonlinear correlations. The concept of producing second-order correlated spectral band images coincides that used to generate covariance function for a random process.

Let $\{B_i\}_{i=1}^{l}$ be the set of all original spectral band images. The first set of second-order statistics spectral band images is generated based on autocorrelation. They are constructed by multiplying each individual spectral band image itself, i.e., $\{B_i^2\}_{i=1}$. A second set of second-order statistics spectral band images are made up of all cross-correlated spectral band images that are produced by correlating any arbitrary two different spectral band images, i.e., $\{B_iB_j\}_{i,j=1,i\neq j}^{l}$. Adding these two sets of second order-statistics spectral band images to $\{B_i\}_{i=1}^{l}$ produces a total of $l+l+(l/2)=(l^2+3l)/2$ spectral band images. In the case where more images are required, nonlinear functions can be used to generate so called nonlinear correlated spectral band images. For example, we may use the square-root or logarithm, i.e., $\{\sqrt{B_i}\}_{i=1}^{l}$ or $\{\log B_i\}_{i=1}^{l}$ to stretch out lower gray-level values. In the following, we describe several ways to generate second-order correlated and nonlinear correlated spectral band images.

1. first-order spectral band image: $\{B_i\}_{i=1}^{l}$ = set of original spectral band images
2. second-order correlated spectral band images

a. $\{B_i^2\}_{i=1}^{l}$ = set of auto-correlated spectral band images

b. $\{B_iB_j\}_{i,j=1,i\neq j}^{l}$ = set of cross-correlated spectral band images

3. Nonlinear correlated spectral band images

a. $\{\sqrt{B_i}\}_{i=1}^{l}$ = set of spectral band images stretched out by the square-root

b. $\{\log B_i\}_{i=1}^{l}$ = set of spectral band images stretched out by the logarithmic function

As noted in DE, all the images generated as just listed are produced nonlinearly. These images should offer useful information for target detection and classification because the classifier to be used for target detection and classification is linear and linearly generated spectral band images will not provide extra new information to help the classifier improve performance.

3 CEM Approach

The CEM approach[7–9] was previously developed for the case that the only required knowledge is the signature of the target to be detected. It used an FIR filter to constrain the desired target signature by a specific gain while minimizing the filter output energy. It was derived from MVDR in sensor array processing[10,11,14] with the desired signature interpreted as the desired direction of signal arrival and can be derived as follows.

Assume that we are given a finite set of observations $S=\{\mathbf{r}_1\mathbf{r}_2\cdots\mathbf{r}_N\}$ where $\mathbf{r}_i=(r_{i1}r_{i2}\cdots r_{il})^T$ for $1\leqslant i\leqslant N$ is a sample pixel vector. Suppose that the desired signature $\mathbf{d}$ is also known *a priori*. The objective of CEM is to design an FIR linear filter with l filter coefficients $\{w_1w_2\cdots w_l\}$, denoted by an l-dimensional vector $\mathbf{w}=(w_1w_2\cdots w_l)^T$ that minimizes the filter output energy subject to the following unity constraint:

$$\mathbf{d}^T\mathbf{w}=\sum_{k=1}^{l} d_kw_k=1. \tag{1}$$

Note that the constraint constant 1 in Eq. (1) can be replaced[11,12] by any scalar c.

Let y_i denote the output of the designed FIR filter resulting from the output $\mathbf{r}_i$. Then y_i can be expressed by

$$y_i=\sum_{k=1}^{l} w_kr_{ik}=\mathbf{w}^T\mathbf{r}_i=\mathbf{r}_i^T\mathbf{w}. \tag{2}$$

Thus, the average output energy produced by the observation set S using the FIR filter with coefficient vector $\mathbf{w}=(w_1w_2\cdots w_L)^T$ specified by Eq. (2) is given by

$$\frac{1}{N}\left[\sum_{i=1}^{N} y_i^2\right]=\frac{1}{N}\left[\sum_{i=1}^{N}(\mathbf{r}_i^T\mathbf{w})^T\mathbf{r}_i^T\mathbf{w}\right]=\mathbf{w}^T\left(\frac{1}{N}\left[\sum_{i=1}^{N}\mathbf{r}_i\mathbf{r}_i^T\right]\right)\mathbf{w}=\mathbf{w}^T\mathbf{R}_{L\times L}\mathbf{w}, \tag{3}$$

where $\mathbf{R}_{l\times l}=(1/N)(\Sigma_{i=1}^{N}\mathbf{r}_i\mathbf{r}_i^T)$ turns out to be the $l\times l$ sample autocorrelation matrix of S.

Minimizing Eq. (3) with the filter response constraint $\mathbf{d}^T\mathbf{w}=\Sigma_{k=1}^{l}d_kw_k=1$ yields

$$\min_{\mathbf{w}}\left\{\frac{1}{N}\left[\sum_{i=1}^{N} y_i^2\right]\right\}=\min_{\mathbf{w}}\{\mathbf{w}^T\mathbf{R}_{l\times l}\mathbf{w}\} \tag{4}$$

subject to $\mathbf{d}^T\mathbf{w}=1$. Solving for Eq. (4) is called CEM approach[7,8] with the weight vector $\mathbf{w}^*$ given by

$$\mathbf{w}^*=\frac{\mathbf{R}_{l\times l}^{-1}d}{\mathbf{d}^T\mathbf{R}_{l\times l}^{-1}\mathbf{d}}. \tag{5}$$

4 GCEM

OSP and CEM have shown success in hyperspectral image classification.[4,7,8] However, when they are applied to multispectral images, both suffer from their small data dimensionality. To expand data dimensions, DE was introduced in GOSP to generate extra spectral band images for the purpose of orthogonal subspace projection. In analogy with GOSP, GCEM also makes use of DE to expand the original multispectral image data to accommodate unknown signal sources such as interferers. Therefore, GCEM is a two-stage process with the first stage carried out by DE, then followed by the second stage, which uses CEM to detect desired targets. A brief description of the procedure implementing GCEM is given as follows.

4.1 *GCEM Algorithm*

1. Apply DE to generate nonlinearly correlated spectral band images.
2. Identify a desired target signature to be detected $\mathbf{d}$.
3. Apply CEM to detect the desired target $\mathbf{d}$.

5 Experimental Results

The data used for the following experiments are the SPOT image with three bands, two of which are from the visible region of electromagnetic spectrum referred to as band 1 (0.5 to 0.59 μm) and band 2 (0.61 to 0.68 μm), and the third band is from the near IR region of electromagnetic spectrum referred to as band 3 (0.79 to 0.89 μm). The ground sampling distance is 20 m. These three bands are shown in Fig. 1. They are registered and combined into an image cube where each pixel is represented by a 3×1 column vector with each component corresponding to one band of the SPOT data. In the scene, there is a river at the bottom left corner. At the center is a large lake and at the right edge are also some small lakes. Between the large lake and many small lakes is a railroad crossing from north to south. Shown at the left of the image scene is an urban area, which has roads and buildings. In addition, there is also a road running on the right edge of the scene. According to the ground truth, there are two large major factories, referred to as ''site a'' (two very bright spots) and ''site b'' (not visible) located at the center of the area. Thus, a total of six target signatures are of interest, two factory sites,

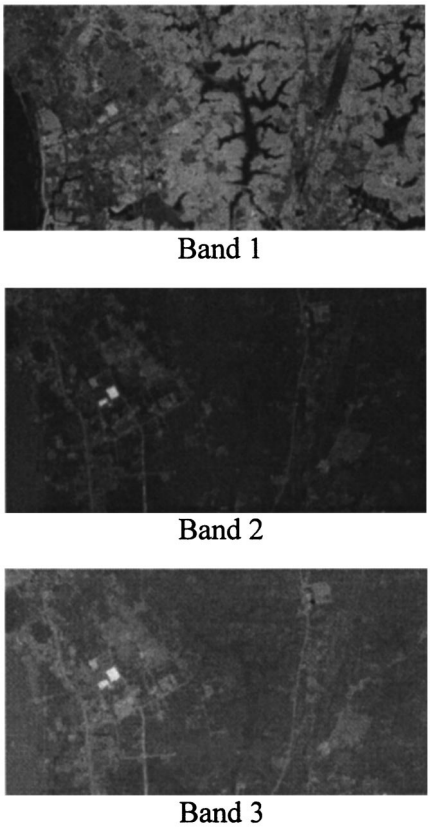

Fig. 1 Three-band SPOT image.

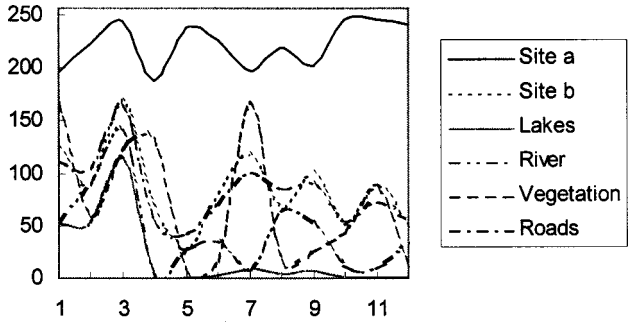

Fig. 2 Six signatures extracted from the image.

''site a'' and ''site b,'' lakes, river, roads, and vegetation and the spectra are shown in Fig. 2. As we can see from Fig. 2, factory ''site a'' has a very distinct spectrum from all the others. Thus, we can expect that it can be easily detected. Figure 3 shows nine images resulting from the DE described in Sec. 2, where the images of Figs. 3(a) to 3(c), 3(d) to 3(f), and 3(g) to 3(i) were obtained by autocorrelation, cross-correlation, and the square root, respectively. Thus combining the 3 original spectral band images in Fig. 1 with those in Fig. 3 results in a total of 12 spectral band images that can be used for GCEM and GOSP. Figures 4 and 5 show the results of GCEM and GOSP, respectively, where the images as labeled as Figs. 4(a) to 4(f) are the detection and classification results of six targets: factory

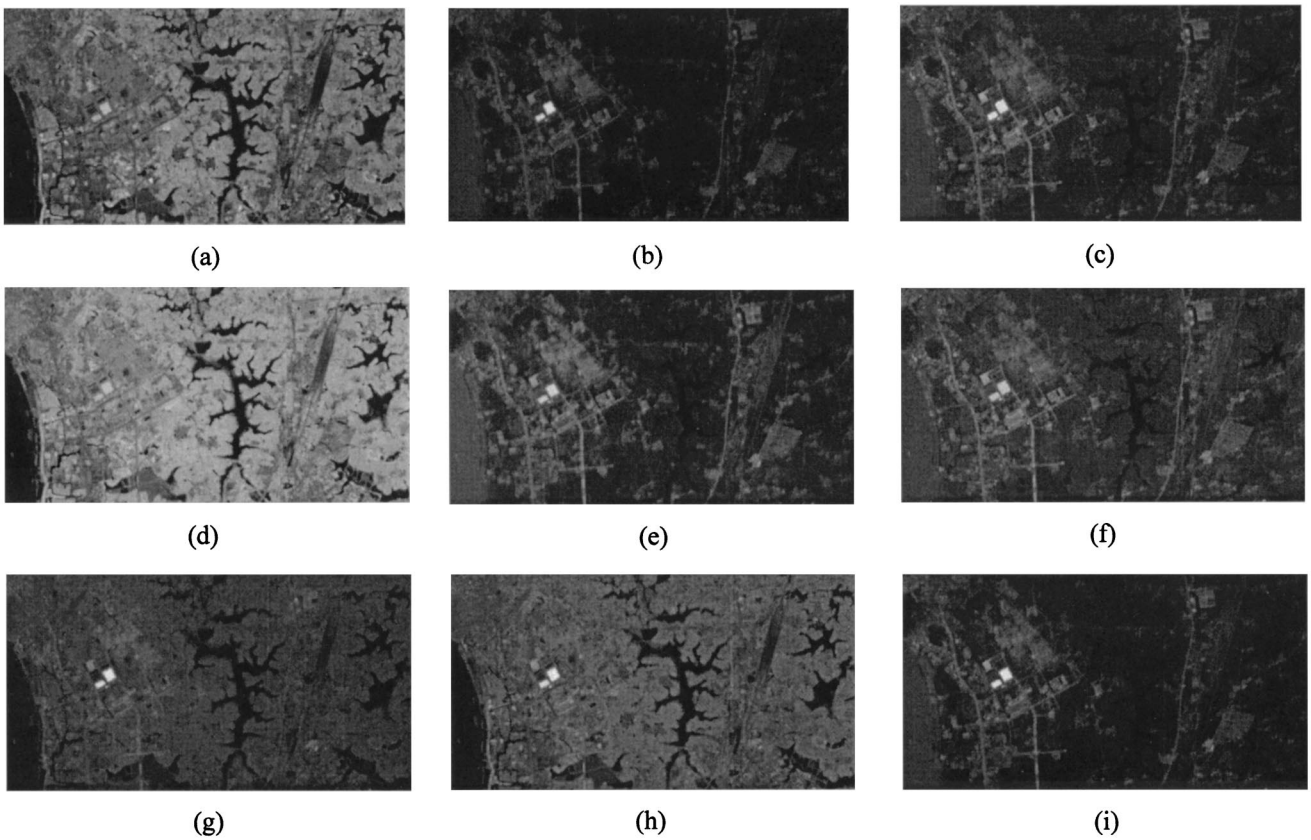

Fig. 3 Nine images resulting from DE where the images (a) to (c), (d) to (f), and (g) to (i) were obtained by autocorrelation, cross-correlation, and the square root, respectively.

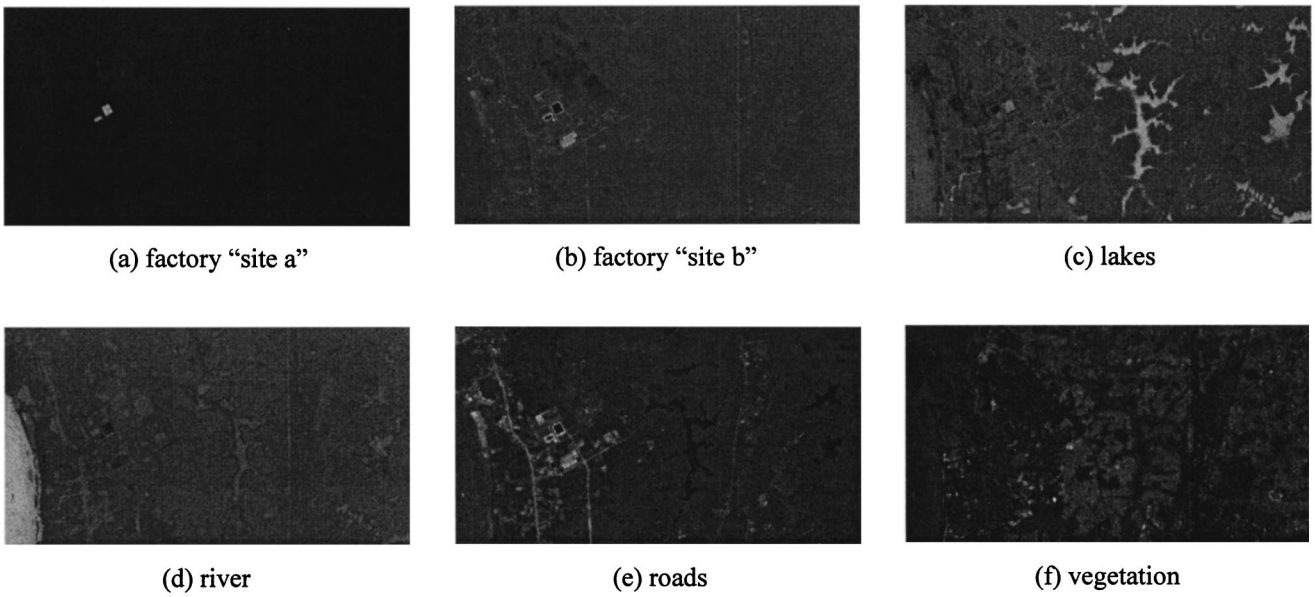

Fig. 4 Classification results of GCEM.

''site a,'' and factory ''site b,'' lakes, river, roads, and vegetation, respectively. Comparing the results in Figs. 4 and 5 GCEM clearly outperformed GOSP in all the cases, particularly for detection and classification of factory ''site b,'' river, and roads. To further demonstrate advantages of GCEM over CEM without using DE, we applied CEM to three original spectral band images in Fig. 1. The detection and classification results are shown in Fig. 6 where the images labeled as Figs. 6(a) to 6(f) are the detection and classification results of factory ''site a,'' factory ''site b,'' lakes, river, roads, and vegetation, respectively. Obviously, GCEM performed significantly better than CEM. For example, CEM failed to detect the factory ''site b'' and had trouble with classifying lakes, river, and roads in Figs. 6(c) to 6(e). This was because their spectra in Fig. 2 were very similar. In addition, from Figs. 5 and 6, it is easy to see that GOSP performed better than CEM in classifying all targets except roads with which GOSP also had trouble. All the preceding experiments demonstrated that to apply hyperspectral image processing techniques such as OSP (Ref. 4) and CEM (Refs. 7, 8) to multispectral imagery data DE is an effective means to extended their applicability and capability. It was noted in Refs. 1 and 3 that OSP performed poorly for SPOT data, which was also the case for the data in Fig. 1. Therefore, the experiments using OSP were not included for comparison.

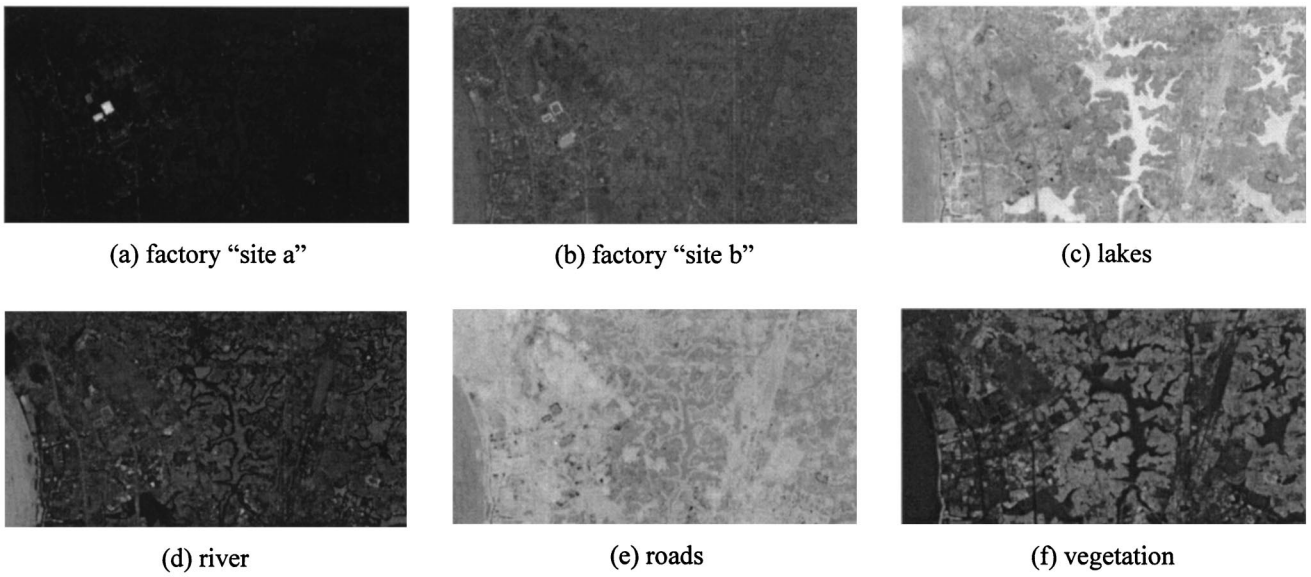

Fig. 5 Classification results of GOSP.

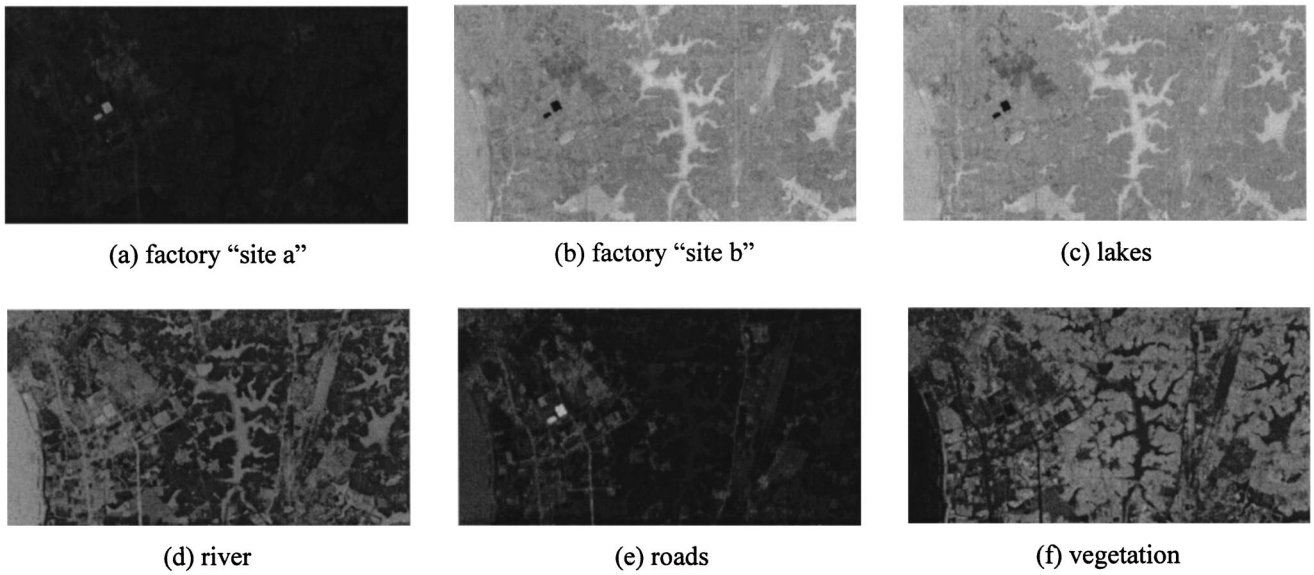

Fig. 6 Classification results of CEM.

6 Conclusion

Despite that CEM has been successfully applied to hyperspectral image classification,[7–9] its applicability to multispectral imagery is yet to be investigated because it has been taken for granted by assuming that CEM will perform as well as it does for hyperspectral imagery. This paper shows that this is not the case. This is so largely due to the fact that CEM suffers from the same problem encountered in the OSP approach,[3,4] that is, data dimensions are insufficient. For CEM to work for multispectral imagery, a GCEM is presented in this paper and can be viewed as a multispectral version of CEM. GCEM incorporates an approach proposed in the GOSP (Ref. 3), DE to expand the original image data so that there are enough spectral band images to make CEM effective. Specifically, GCEM is a two-stage process with the first stage implemented by DE to expand image data, then followed by using CEM in the second stage. The experiments show that GCEM overcomes the inherent limitation of CEM on data dimensionality and performs significantly better than CEM without using DE. This is so because the spectral band images generated by DE are nonlinearly correlated images that provide useful information to improve CEM performance. Additional experiments also show that GCEM outperforms GOSP since GCEM requires only the knowledge of the desired target signature rather than the complete knowledge of target signatures in the image scene required for GOSP, a situation that is rarely satisfied in many real applications. However, like CEM, GCEM is very sensitive to noise and the used desired target signature. Recently, this problem is alleviated by an approach proposed in Ref. 12, called the LCMV method, which constrains multiple target signatures instead of a single desired target signature. As a result, LCMV performs more robustly than CEM. By taking advantage of LCMV, GCEM can be further extended to GLCMV.

References

1. C.-I. Chang and C. Brumbley, ''A Kalman filtering approach to multispectral image classification and detection of changes in signature abundance,'' *IEEE Trans. Geosci. Remote Sens.* **37**(1), 257–268 (1999).
2. S. S. Epp, *Discrete Mathematics with Application*, 2nd ed., Brooks/Cole Publishing (1995).
3. H. Ren and C.-I. Chang, ''Generalized orthogonal subspace projection approach to unsupervised multispectral image classification,'' *Proc. SPIE* **3500**, pp. 42–53, Spain (1998).
4. J. Harsanyi and C.-I. Chang, ''Hyperspectral image classification and dimensionality reduction: an orthogonal subspace projection approach,'' *IEEE Trans. Geosci. Remote Sens.* **32**, 779–785 (1994).
5. J. J. Settle, ''On the relationship between spectral unmixing and subspace projection,'' *IEEE Trans. Geosci. Remote Sens.* **34**, 1045–1046 (1996).
6. C.-I. Chang, ''Further results on relationship between spectral unmixing and subspace projection,'' *IEEE Trans. Geosci. Remote Sens.* **36**(3), 1030–1032 (1998).
7. J. C. Harsanyi, ''Detection and classification of subpixel spectral signatures in hyperspectral image sequences,'' PhD Dissertation, Department of Electrical Engineering, University of Maryland Baltimore County Baltimore (1993).
8. J. C. Harsanyi, W. Farrand, and C.-I. Chang, ''Detection of subpixel spectral signatures in hyperspectral image sequences,'' in *Proc. Annu. M. Am. Soc. Photogrammetry and Remote Sensing*, pp. 236–247, Reno (1994).
9. W. Farrand and J. C. Harsanyi, ''Mapping the distribution of mine tailing in the coeur d'Alene river valley, Idaho, through the use of constrained energy minimization technique,'' *Remote Sens. Environ.* **59**, 64–76 (1997).
10. O. L. Frost III, ''An algorithm for linearly constrained adaptive array processing,'' *Proc. IEEE* **60**, 926–935 (1972).
11. B. D. Van Veen and K. M. Buckley, ''Beamforming: a versatile approach to spatial filtering,'' *IEEE ASSP Mag.* , 4–24 (Apr. 1998).
12. C.-I. Chang and H. Ren, ''Linearly constrained minimum variance beamforming for target detection and classification in hyperspectral imagery,'' in *IEEE Int. Geoscience and Remote Sensing Symp. '99*, pp. 1241–1243, Hamburg, Germany (1999).
13. H. Ren, ''A comparative study of mixed pixel classification versus pure pixel classification for multi/hyperspectral imagery,'' M S Thesis, Department of Computer Science and Electrical Engineering, University of Maryland Baltimore County, Baltimore (May 1998).
14. S. Haykin, *Adaptive Filter Theory*, 3rd. ed., Prentice-Hall, Englewood Cliffs, NJ (1996).

Chein-I Chang received his BS, MS, and MA degrees from Soochow University, Taipei, Taiwan, in 1973, the Institute of Mathematics at National Tsing Hua University, Hsinchu, Taiwan, in 1975, and the State University of New York at Stony Brook, 1977, respectively, all in mathematics, his MS and MSEE degrees from the University of Illinois at Urbana-Champaign in 1982, respectively, and his PhD in electrical engineering from the University of Maryland, College Park, in 1987. He was a visiting assistant professor from January 1987 to August 1987, assistant professor from 1987 to 1993, and is currently an associate professor in the Department of Computer Science and Electrical Engineering at the University of Maryland, Baltimore County. He was a visiting specialist in the Institute of Information Engineering at the National Cheng Kung University, Tainan, Taiwan, from 1994 to 1995. His research interests include automatic target recognition, multispectral/hyperspectral image processing, medical imaging, information theory and coding, signal detection and estimation, and neural networks. Dr. Chang is a senior member of IEEE and a member of SPIE, INNS, Phi Kappa Phi, and Eta Kappa Nu.

Jih-Ming Liu received his BSEE and MSEE degrees from Chung Cheng Institute of Technology, Taipei, Taiwan, in 1987 and 1992, respectively. He is currently pursuing his PhD degree at the National Taiwan University of Science and Technology. His research interests include remote sensing, signal/image processing, neutral networks, and statistical pattern recognition.

Bin-Chang Chieu received his PhD degree in electrical engineering from Rensselaer Polytechnic Institute, Troy, New York, in 1989. He is currently a professor in the Department of Electronic Engineering, National Taiwan University of Science and Technology, Taipei, Taiwan. His current research interests are image processing, digital signal processing, neural networks, and computer vision.

Hsuan Ren received his BS degree in electrical engineering from the National Taiwan University, Taipei, Taiwan, in 1994 and his MS degree in computer science and electrical engineering from University of Maryland, Baltimore County, in 1998, where he is currently a PhD candidate. He is currently a research assistant in the Remote Sensing, Signal and Image Processing Laboratory, University of Maryland, Baltimore County. His research interests include data compression, signal and image processing, and pattern recognition. He is also a member of Phi Kappa Phi.

Chuin-Mu Wang received his BS degree in electronic engineering from National Taipei Institute of Technology and his MS degree in information engineering from Tatung University of Taiwan in 1984 and 1990, respectively. From 1984 to 1990, he was a system programmer on an IBM mainframe system and from 1990 to 1992 he was a marketing engineer on computer products at Tatung Company. Since 1992, he has been a lecturer at the Chinyi Institute of Technology. His research interests include database, digital image process, and neural network.

Chien-Shun Lo received his BS and MS degrees in information engineering and computer science from Feng-Chia University, Taiwan, in 1992 and 1994, respectively. He is now working toward a PhD degree at the Institute of Electrical Engineering, National Cheng-Kung University, Taiwan. He is also a research assistant in the Department of Radiology, Taichung Veterans General Hospital, Taiwan. His current research interests are image processing, medical image processing and analysis, and computer-aided diagnostic system.

Pau-Choo Chung received her BS and MS degrees in electrical engineering from National Cheng Kung University, Tainan, Taiwan, in 1981 and 1983, respectively, and her PhD degree in electrical engineering from Texas Tech University, Lubbock, in 1991. From 1983 to 1986, she was with the Chung Shan Institute of Science and Technology, Taiwan. Since 1991, she has been with the Department of Electrical Engineering, National Cheng Kung University, where she is currently a full professor. Her current research includes neural networks and their applications to medical image processing, medical image analysis, telemedicine, and video image analysis.

Chin-Wen Yang received his BS degree in information engineering sciences from Feng-Chia University, Taiwan, in 1987 and his MS degree in information engineering in 1989 and his PhD degree in electrical engineering in 1996 from National Cheng Kung University, Taiwan. He is currently a system management chief in the Computer and Communication Center at Taichung Veterans General Hospital, Taiwan. His research interests include image processing, biomedical image processing, and computer network.

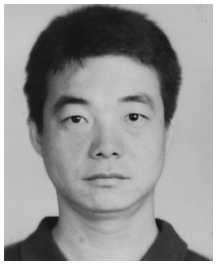

Dye-Jyun Ma received his BS degree in electronics engineering from National Chiao-Tung University, Taiwan, in 1979 and has MS and PhD degrees in electrical engineering from the University of Maryland, College Park, in 1984 and 1988, respectively. From May 1988 to June 1993, he was with Digital Equipment Corporation, Massachusetts, as a principal engineer, where he was responsible for performance modeling and analysis of computer communication networks. Since August 1993, he has been with the Department of Electrical Engineering, National Chung-Hsing University, Taichung, Taiwan, where he is presently a professor and chairs the department. His research interests include stochastic control and optimization, modeling and optimal design of communication networks, remote sensing, and medical image processing.